Multimodality Imaging of Neurodegenerative Processes: Part 2, Atypical Dementias

Erica L. Martin-Macintosh[1]
Stephen M. Broski[1]
Geoffrey B. Johnson[1]
Christopher H. Hunt[1,2]
Ethany L. Cullen[1]
Patrick J. Peller[1,3]

OBJECTIVE. The purpose of this article is to describe the role of multimodality imaging in the evaluation of atypical neurodegenerative conditions. An imaging approach to the more common dementia disease processes was described in part 1. This article, part 2, briefly discusses current Centers for Medicare & Medicaid Services coverage for imaging patients with dementia and illustrates the basic concepts of combining anatomic, metabolic, and amyloid imaging in the evaluation of patients with atypical neurodegenerative dementia. Although these disease processes are rare, the growing repertoire of clinically available imaging techniques necessitates an understanding of their imaging patterns.

CONCLUSION. Despite the rarity of these conditions, imaging of patients with neurodegenerative disorders is on the rise, and familiarity with the imaging appearances of these atypical causes is increasingly important.

Keywords: brain, dementia, molecular imaging, neurodegenerative

DOI:10.2214/AJR.14.12910

Received March 18, 2014; accepted after revision February 6, 2016.

Based on a presentation at the ARRS 2013 Annual Meeting, Washington, DC.

[1]Department of Radiology, Division of Nuclear Radiology, Mayo Clinic, 200 First St SW, Rochester, MN 55905. Address correspondence to E. L. Martin-Macintosh (martinmacintosh.erica@gmail.com).

[2]Department of Radiology, Division of Neuroradiology, Mayo Clinic, Rochester, MN.

[3]Eka Medical Center Jakarta, Bumi Serpong Damai City, Tangerang, Indonesia.

AJR 2016; 207:883–895

0361–803X/16/2074–883

Progress in anatomic and metabolic imaging, as described in part 1 [1], has led to a multimodality approach for imaging patients with cognitive decline. Although the combination of Alzheimer disease (AD), frontotemporal dementia (FTD), vascular dementia, and dementia with Lewy bodies (DLB), which are discussed in part 1 [1], accounts for at least 85% of the degenerative dementias, the remainder is significant. These atypical degenerative dementias have varied clinical presentations, prognoses, and treatments. As a result, correct diagnosis is essential for proper patient care and education.

The major international radiology societies have recognized the importance of multimodality imaging in these atypical cases. The current American College of Radiology Appropriateness Criteria for dementia and movement disorders recommends advanced anatomic imaging in all patients while reserving FDG and amyloid PET/CT for problem-solving purposes, such as those commonly encountered in atypical degenerative dementias [2, 3]. Nevertheless, the Centers for Medicare & Medicaid Services (CMS) currently reimburses for only a single technically adequate FDG PET/CT examination of patients with presumed, probable, or uncertain AD when an alternate diagnosis of FTD is being considered. More specifically, these patients must meet the diagnostic criteria of both diseases with documented cognitive decline for at least 6 months. Clinical suspicion must be aided by cognitive scales, neuropsychology testing, laboratory tests, and anatomic imaging with CT or MRI [3]. Although the U.S. Food and Drug Administration has approved three amyloid imaging agents (^{18}F-florbetapir, ^{18}F-flutemetamol, and ^{18}F-florbetaben) and their utility has been described in characterizing early AD and several other dementia subtypes, amyloid PET is not reimbursed by CMS [4]. However, the use of metabolic and amyloid imaging for both atypical and typical causes of dementia continues to evolve in both the research and clinical arenas. Given the considerable clinical overlap with the more common dementias, familiarity with the imaging appearances of atypical dementias is necessary.

The purpose of this article is to build on the reader's knowledge of the classic anatomic and metabolic appearances of the more common degenerative dementias and apply those same principles to the uncommon—but clinically important—subset of atypical degenerative dementias.

Imaging Techniques

Standardized imaging protocols for both anatomic and metabolic imaging of the brain are essential for reliable and accurate diagno-

TABLE 1: Typical Imaging Patterns of Less Common Neurodegenerative and Dementialike Processes

Process	MRI	^{18}F-FDG PET	Amyloid PET
Corticobasal degeneration	Asymmetric (most commonly left-sided) but affecting contralateral side of clinical symptoms Asymmetric in 50% of cases	Asymmetric (most commonly left-sided) but affecting contralateral side of clinical symptoms ↓ Parietal and to a lesser extent frontal cortex ↓ Basal ganglia	May be positive in patients with Alzheimer disease subtype
Multiple-system atrophy	"Slit void" sign "Hot cross bun" sign	↓ Striatum (MSA-P) ↓ Brainstem and cerebellum (MSA-C)	Normal
Progressive supranuclear palsy	"Hummingbird" sign "Mickey Mouse" sign	↓ Posterior frontal lobe, midbrain, basal ganglia	Normal
Pseudodementia	Normal	Normal (most common) Diffusely ↓ (less common)	Normal
Paraneoplastic syndrome	Atrophy Abnormal T2 signal and/or enhancement	Variable depending on pattern of involvement and phase (acute versus chronic/treated) ↑ Anterior temporal (limbic encephalitis) ↓ or ↑ Cerebellum (cerebellar degeneration)	Normal
Creutzfeldt-Jakob disease	Thalamus: increased T2 signal and diffusion restriction Gyriform: increased T2 signal and enhancement Rapid frontotemporal lobe atrophy	Regional hypometabolism	Normal
Huntington disease	Caudate and basal ganglia atrophy	↓ Basal ganglia (precedes symptoms but better seen with ^{11}C-raclopride) ↓ Frontotemporal lobe	Normal

Note—Downward-pointing arrow (↓) = decreased metabolism, MSA-P = multiple-system atrophy with predominantly parkinsonism symptoms, MSA-C = multiple-system atrophy with predominantly cerebellar ataxia symptoms, upward-pointing arrow (↑) = increased metabolism.

sis of degenerative dementias and for longitudinal studies evaluating disease progression in both the clinical and research realms. Protocols for anatomic and metabolic imaging with MRI and PET/CT were described in part 1 [1]. To summarize briefly, detailed anatomic imaging with MRI is preferable to CT because of MRI's increased sensitivity. Traditional MRI sequences including sagittal T1-weighted, axial T2-weighted, axial FLAIR, and DWI sequences should be considered the bare minimum for an adequate evaluation. These sequences are frequently augmented by a 3D volumetric T1-weighted acquisition to give a more accurate qualitative or quantitative measurement of focal atrophy [5]. Gradient-recalled echo or susceptibility-weighted images along with gadolinium-enhanced images are also frequently used.

Metabolic imaging with ^{18}F-FDG (FDG) PET/CT remains the main staple of metabolic imaging. Dedicated brain acquisition, as described in part 1 [1], can provide a reliable and reproducible means to measure cortical glucose metabolism, which is essential in characterizing degenerative dementias [6]. The addition of a semiquantitative analysis is a relatively simple way to significantly increase both sensitivity and specificity [7] and at our institution is considered the standard of care both by the interpreting physician and by the referring clinicians. Quantitative programs sample the FDG PET dataset at thousands of cortical locations to create a 3D stereotactic surface projection (SSP). An age-matched Z-score can be generated for each cortical region by comparing with a normative database on a voxel-by-voxel basis. The Z-score data can then be displayed on 3D SSP brain surface maps for visual inspection [8].

Amyloid PET/CT has gained an increasing role for clinical evaluation of degenerative dementias. The current appropriate use criteria from the Amyloid Imaging Taskforce, a joint effort of the Alzheimer's Association and the Society of Nuclear Medicine and Molecular Imaging, states that amyloid PET should be considered in patients when there is significant diagnostic uncertainty after comprehensive evaluation and when the results are anticipated to increase diagnostic certainty and alter management [9, 10].

Atypical Degenerative Dementias

The atypical degenerative dementias are an unusual collection of disease processes that are typically more aggressive than the disorders discussed in part 1 [1]. The initial clinical presentation of atypical degenerative dementias can often be confusing, and both prognostication and symptomatic management can be greatly aided by accurate diagnosis with the help of anatomic and metabolic imaging (Table 1).

Corticobasal Degeneration

Corticobasal degeneration (CBD) is characterized by cognitive decline or behavioral disturbance that precedes the development of a movement disorder, typically asymmetric parkinsonism or alien limb phenomenon [11–14]. Specific cognitive features include executive dysfunction, aphasia, apraxia, and visuospatial disturbances. Similar to the parkinsonism of many other atypical degener-

ative dementias, parkinsonism in CBD can be differentiated from idiopathic Parkinson disease in that it is typically asymmetric and lacks a robust response to levodopa therapy [15]. Current research suggests that CBD may be further divided into FTD and AD subtypes on the basis of the underlying histology at autopsy [12]. Although not robust, dopaminergic drugs may be helpful for symptom treatment. Targeted therapy with botulinum toxin for symptomatic limb dystonia can also improve quality of life [16]. A relatively aggressive course is typically seen, with a mean survival of 8 years from symptom onset [14].

Anatomic imaging—In the early stages of CBD, the MRI findings may be subtle. With disease progression, asymmetric cortical atrophy involving the frontoparietal lobes and corpus callosum may be present (Fig. 1A). There may also be atrophy of the ipsilateral cerebellar peduncle. On T2-weighted sequences, marked hypointensity can be seen in the putamen and globus pallidum. Volume loss does not occur in the basal ganglia and hippocampi, which can be helpful in differentiation from AD [17–19].

Metabolic imaging—FDG PET/CT classically shows asymmetric basal ganglia and cortical hypometabolism contralateral to the patient's affected side (Figs. 1B–1D). Frequently this is manifested by left-sided cerebral hypometabolism in the context of right-sided symptoms [20, 21]. The parietal and, to a lesser extent, frontal lobes are frequently involved early in the disease process. Interestingly, studies have revealed hypermetabolism in the basal ganglia and cortex ipsilateral to the clinically affected side [21].

Amyloid imaging—The AD subtype of CBD theoretically may show a pattern of amyloid deposition similar to that of AD. However, the prevalence of amyloid-positive CBD is not yet known [12].

Multiple-System Atrophy

Like CBD, multiple-system atrophy (MSA) is a neurodegenerative movement disorder characterized by prominent parkinsonism. Cognitive decline and cerebellar ataxia with early falls are characteristic of this disorder. When dysautonomia predominates, this condition may be termed "Shy-Drager syndrome." This disease process is further subclassified on the basis of the type of movement disorder: MSA with predominantly parkinsonism symptoms is referred to as "MSA-P," and MSA with predominantly cerebellar ataxia symptoms is referred to as "MSA-C" [22]. Dopamine replacement therapy is not beneficial in patients with MSA, unlike patients with CBD, and can potentially aggravate the dysautonomia. As with the other atypical degenerative dementias, the clinical course of MSA is aggressive, and death typically occurs within 10 years of diagnosis. In patients with prominent dysautonomia, the prognosis can be even worse.

Anatomic imaging—Multiple distinct patterns may be seen on conventional MRI of patients with MSA. In MSA-P, putaminal abnormalities predominate with atrophy and symmetric hypointensity on T2-weighted and gradient-weighted images [22]. Nevertheless, this putaminal T2 hypointensity is nonspecific and may also be seen with progressive supranuclear palsy (PSP), Wilson disease, iron deposition, and other acquired conditions [23]. A slitlike T2 marginal hyperintensity may also be seen in the putamen; however, this finding has also been identified in healthy patients studied with 3-T magnets [24]. In patients with MSA-C, atrophy of the inferior basis pontis, medulla, middle cerebellar peduncles, and cerebellar hemispheres with associated widening of the fourth ventricle may be seen [23]. These patients may show the classic triad cruciform T2 signal in the pons termed the "hot cross bun" sign. This sign represents focal loss of pontine neurons and transverse pontocerebellar fibers [25] (Fig. 2A). In combination, these structural findings are relatively specific for the subtypes of MSA, but detection of these findings on imaging in early disease is suboptimal.

Metabolic imaging—FDG PET/CT may reveal striatal, brainstem, and cerebellar hypometabolic patterns that mirror the regions of structural atrophy and T2 signal abnormalities on MRI. Specifically, patients with MSA-P may show putaminal hypometabolism, and patients with MSA-C may show cerebellar and middle cerebellar peduncle hypometabolism [20] (Figs. 2B–2D). However, patients with MSA-P without cerebellar symptoms may also have cerebellar hypometabolism [26].

Amyloid imaging—Patients with MSA show no amyloid deposition on amyloid PET.

Progressive Supranuclear Palsy

PSP is clinically characterized by parkinsonism, postural instability, and vertical gaze palsy. PSP is the second most common cause of parkinsonism after idiopathic Parkinson disease. PSP is characterized by early falls within the first year of disease onset, and there is typically symmetric involvement at presentation with central (i.e., trunk and neck) involvement greater than limb involvement. Although supranuclear ophthalmoplegia is the most striking cranial nerve finding, other cranial nerves can also be involved, producing pseudobulbar palsy and cervical dystonia [27]. Concomitant cognitive impairment is typically characterized by personality change, memory impairment, and depression or apathy [22, 28]. Disease progression is usually aggressive, with death occurring within 6–10 years of diagnosis. Misdiagnosis as idiopathic Parkinson disease is not rare, and this misdiagnosis may lead to unnecessary trials of dopamine replacement therapy, to which PSP is typically unresponsive.

Anatomic imaging—Three abnormalities have been classically described in PSP on conventional MRI. These abnormalities include the following: first, atrophy of the midbrain tegmentum with relative preservation of the pons, which is termed the "hummingbird" sign, on midline sagittal images [29]; second, atrophy of the midbrain, preservation of the tectum, and widening of the interpeduncular cistern, which is termed the "Mickey Mouse" sign, on axial images [30]; and putaminal T2 hypointensity, which is likely caused by iron deposition [31] (Fig. 3A). Additional findings that may assist in differentiating PSP from other neurodegenerative processes include atrophy and abnormal FLAIR signal intensity of the cerebellar peduncles [32].

Metabolic imaging—FDG PET/CT may reveal posterior frontal cortex, midbrain, and basal ganglia hypometabolism [20, 26, 28] (Figs. 3B–3D). A predilection for involvement of the midline structures may be seen, particularly the parasagittal frontal lobes [27]. Like hypometabolism seen in patients with AD, hypometabolism in patients with PSP typically spares the motor and sensory cortex until late in the disease process.

Amyloid imaging—PSP is characterized by accumulation of phosphorylated tau protein in the brain. No amyloid deposition has been shown on amyloid PET in the setting of PSP.

Pseudodementia

Pseudodementia has been described as a reversible dementia syndrome secondary to a primary psychiatric disorder, classically major depressive disorder. This diagnosis should be considered in the differential diagnosis of any patient with a long-standing psychiatric history. Clinically, the only major differentiating factor is the complete reversibility of the symptoms after treatment. In the popula-

tion with treatment-resistant major depressive disorder, cognitive symptom improvement may be achieved only after electroconvulsive therapy (ECT) [33]. Significant morbidity and mortality can be associated with this condition, which stresses the importance of early and accurate diagnosis.

Anatomic imaging—No structural or morphologic abnormalities are seen on conventional MRI in pseudodementia. However, this lack of structural abnormalities may be indistinguishable from other early-stage dementia processes.

Metabolic imaging—A broad spectrum of presentations may be seen on FDG PET/CT; most commonly, FDG PET/CT of these patients will show normal metabolism (Fig. 4). However, diffuse hypometabolism has also been described [34], and there have been several cases reported of severe depressive pseudodementia with diffuse cerebral hypometabolism showing varying degrees of metabolic change after ECT. Findings include immediate progression of hypometabolism, complete resolution [35], and minimal change despite clinical improvement [36] after ECT. The overlapping appearance of pseudodementia with that of neurodegenerative disease on FDG PET/CT has the potential to lead to misinterpretation in the setting of depression [35]. This possibility should be kept in mind when interpreting FDG PET/CT studies of patients with a significant psychiatric history.

Amyloid imaging—No amyloid deposition has been detected on amyloid PET in the setting of pseudodementia.

Paraneoplastic Neurological Syndromes

Paraneoplastic neurological syndromes (PNS) are a rare group of disorders that result from neuronal dysfunction in the setting of malignancy that is likely because of immune-mediated direct damage rather than because of metastasis, infection, metabolic deficits, or treatment [37]. This phenomenon is most frequently encountered in breast, lung, and ovarian cancer and is estimated to occur in less than 0.01% of patients with cancer [38]. Most often, the symptoms of PNS develop before the detection of the primary malignancy [38]. There are multiple syndromes included in the PNS that may present clinically with cognitive symptoms; two of the more common entities include paraneoplastic limbic encephalitis and subacute cerebellar degeneration [39]. Patients with paraneoplastic limbic encephalitis, the most common clinical paraneoplastic syndrome, present with cognitive decline, confusion, and possibly seizures. Patients with subacute cerebellar degeneration typically present with profound axial and appendicular ataxia, dysarthria, and nystagmus. Accurate diagnosis can help to initiate treatment with immune-modulating therapies and elicit a search for occult malignancy in these patients.

Anatomic imaging—Conventional MRI findings may range from grossly normal to abnormal in PNS. Paraneoplastic limbic encephalitis can mimic herpes encephalitis on imaging with relatively symmetric T2 hyperintensity in the medial temporal lobes. The cingulate gyrus, insula, inferior frontal cortex, and white matter may be involved as well [40]. Minimal mass effect and patchy contrast enhancement can be present, which may confuse the imaging appearance (Fig. 5A). In acute cases in which herpes cannot be excluded, treatment with antiviral agents is advised until herpes encephalitis can be excluded by spinal fluid examination. In paraneoplastic cerebellar degeneration, focal atrophy of the cerebellum is noted. This disorder can be difficult to accurately diagnose in patients with more widespread cerebral atrophy, but there is progressive volume loss on serial examinations [41]. The cerebellar atrophy is often more obvious on sagittal images than on axial images.

Metabolic imaging—Several patterns of altered cerebral metabolism have been described in PNS. In a recent study, investigators reported that approximately 63% of patients with PNS will show some degree of abnormality on FDG PET/CT [37]. In paraneoplastic limbic encephalitis, increased glucose metabolism is typically seen in the active phases of the disease, and glucose metabolism may be useful in monitoring response to treatment (Figs. 5B–5D). In paraneoplastic cerebellar degeneration, marked cerebellar hypometabolism and less commonly hypermetabolism have been noted. This metabolic abnormality is often more pronounced and, expecially with quantitation, is easier to detect than cerebellar atrophy. Following treatment of the underlying malignancy, cerebral hypometabolism often develops in the involved areas in hypermetabolism that was previously present [37].

Amyloid imaging—No amyloid deposition has been shown on amyloid PET in the setting of PNS.

Creutzfeldt-Jakob Disease

Creutzfeldt-Jakob disease (CJD) is a rare fatal prion neurodegenerative disease characterized by rapidly progressive dementia with myoclonus. Although there are classic pathologic findings on brain biopsy, noninvasive diagnosis by a combination of electroencephalography (EEG) and imaging findings is optimal to reduce the potential for additional potential prion exposures. In addition to characteristic EEG periodic complexes, highly specific features can be seen on imaging that allow accurate diagnosis of CJD [42].

Anatomic imaging—The most common imaging finding is rapidly progressive atrophy that typically involves the frontal, temporal, and parietal lobes. Rarer subtypes can preferentially involve the occipital (Heidenhain variant) and cerebellar (Oppenheimer-Brownell variant) hemispheres [43, 44]. Aside from the progressive atrophy (Figs. 6A and 6B), more specific MRI features can be present and include, first, T2 signal and diffusion restriction in the pulvinar of the thalami; and, second, symmetric increased signal intensity in the pulvinar and dorsomedial thalamus that gives a "hockey stick" configuration [45]. Other findings frequently encountered include patchy gyriform T2 hyperintensity in the cerebral cortex and increased T1 signal in the globus pallidum [42] (Figs. 6C–6E).

Molecular imaging—Although a classic appearance of CJD has not been described on FDG PET/CT, cases of regional hypometabolism in patients with CJD have been reported that could easily lead to misdiagnosis of CJD as CBD or DLB. In these cases, the rapid progression of the clinical and imaging findings ultimately led to the diagnosis of CJD [46].

Amyloid imaging—No amyloid deposition has been shown on amyloid PET in the setting of CJD.

Huntington Disease

Huntington disease (HD) is an uncommon autosomal-dominant neurodegenerative disease with both juvenile and adult-onset forms that is characterized by cytosine-adenosine-guanine trinucleotide repeats in the short arm of chromosome 4 [47, 48]. The classic adult-onset form, accounting for approximately 90–95% of HD cases, typically presents in patients 40–50 years old with rapidly progressive mental deterioration and choreoathetoid movements [49]. The less common juvenile form typically presents in patients younger than 20 years old, and affected patients can have prominent rigidity [47]. Although HD is autosomal-dominant, approximately 10–15% of cases are sporadic, which can potentially lead to a delayed diagnosis [50].

Anatomic imaging—The main feature of HD is caudate atrophy with overall decreased size, loss of the convex medial margin of the caudate heads, and an increased intercaudate distance (Figs. 7A and 7B). Putaminal and globus pallidus volume loss with compensatory enlargement of the anterior horns of the lateral ventricles may also be seen. The basal ganglia atrophy can be subtle, especially in minimally symptomatic patients or in presymptomatic patients [51]. Therefore, volumetric quantitation may be useful. Nonspecific T2 hypointensity in the striatum can result from iron deposition. In the juvenile form, T2 hyperintensity in the caudate and putamen may occur due to gliosis [47, 48, 52].

Molecular imaging—FDG PET typically shows hypometabolism in the frontal and temporal lobes and more severe deficits in the basal ganglia (Figs. 7C and 7D). These metabolic abnormalities can be identified in patients with HD many years before the onset of clinical symptoms [53, 54]. Some sources suggest that decreased cortical glucose metabolism is a predictor for more rapid HD progression [55, 56]. Imaging with less common PET radiotracers such as ^{11}C-raclopride, a D2 dopamine antagonist, can detect even subtler alterations in basal ganglia function and may be used to prognosticate disease severity and correlate with the number of trinucleotide repeats [57] (Figs 7E and 7F).

Amyloid imaging—No amyloid deposition has been reported on amyloid PET in the setting of HD.

Conclusion

In part 1 [1], we discussed multimodality imaging of the most common neurodegenerative causes of dementia. In part 2, we build on the reader's knowledge by describing less common causes of degenerative dementia and illustrate the complementary roles of anatomic, metabolic, and sometimes amyloid imaging. Despite the rarity of these conditions, imaging of patients with neurodegenerative disorders is on the rise, and familiarity with the imaging appearances of these atypical causes is increasingly important.

Acknowledgments

We thank Sonia Watson and Andrea Moran for their assistance with the preparation and editing of our manuscript.

References

1. Martin-Macintosh EL, Broski SM, Johnson GB, Hunt CH, Cullen EL, Peller PJ. Multimodality imaging of neurodegenerative processes. Part 1. The basics and common dementias. *AJR* 2016; 207:871–882
2. Dormont D, Seidenwurm DJ. Dementia and movement disorders. *AJNR* 2008; 29:204–206
3. American College of Radiology website. ACR Appropriateness Criteria: dementia and movement disorders. https://acsearch.acr.org/docs/69360/Narrative/. Accessed December 8, 2014
4. Centers for Medicare & Medicaid Services website. National coverage determination (NCD) for FDG PET for dementia and neurodegenerative diseases (220.6.13). www.cms.gov/medicare-coverage-database/details/ncd-details.aspx?NCDId=288&ncdver=3&bc=BAABAAAAAAAA&. Published 2009. Accessed December 8, 2014
5. Jack CR Jr. Alzheimer disease: new concepts on its neurobiology and the clinical role imaging will play. *Radiology* 2012; 263:344–361
6. Minoshima S. Imaging Alzheimer's disease: clinical applications. *Neuroimaging Clin N Am* 2003; 13:769–780
7. Lehman VT, Carter RE, Claassen DO, et al. Visual assessment versus quantitative three-dimensional stereotactic surface projection fluorodeoxyglucose positron emission tomography for detection of mild cognitive impairment and Alzheimer disease. *Clin Nucl Med* 2012; 37:721–726
8. Minoshima S, Frey KA, Koeppe RA, Foster NL, Kuhl DE. A diagnostic approach in Alzheimer's disease using three-dimensional stereotactic surface projections of fluorine-18-FDG PET. *J Nucl Med* 1995; 36:1238–1248
9. Sánchez-Juan P, Ghosh PM, Hagen J, et al. Practical utility of amyloid and FDG-PET in an academic dementia center. *Neurology* 2014; 82:230–238
10. Johnson KA, Minoshima S, Bohnen NI, et al.; Alzheimer's Association; Society of Nuclear Medicine and Molecular Imaging; Amyloid Imaging Taskforce. Appropriate use criteria for amyloid PET: a report of the Amyloid Imaging Task Force, the Society of Nuclear Medicine and Molecular Imaging, and the Alzheimer's Association. *Alzheimers Dement* 2013; 9:e-1–e-16
11. Graham NL, Bak TH, Hodges JR. Corticobasal degeneration as a cognitive disorder. *Mov Disord* 2003; 18:1224–1232
12. Lee SE, Rabinovici GD, Mayo MC, et al. Clinicopathological correlations in corticobasal degeneration. *Ann Neurol* 2011; 70:327–340
13. Murray R, Neumann M, Forman MS, et al. Cognitive and motor assessment in autopsy-proven corticobasal degeneration. *Neurology* 2007; 68:1274–1283
14. Wenning GK, Litvan I, Jankovic J, et al. Natural history and survival of 14 patients with corticobasal degeneration confirmed at postmortem examination. *J Neurol Neurosurg Psychiatry* 1998; 64:184–189
15. McGinnis SM. Neuroimaging in neurodegenerative dementias. *Semin Neurol* 2012; 32:347–360
16. Stamelou M, Alonso-Canovas A, Bhatia KP. Dystonia in corticobasal degeneration: a review of the literature on 404 pathologically proven cases. *Mov Disord* 2012; 27:696–702
17. Savoiardo M. Differential diagnosis of Parkinson's disease and atypical parkinsonian disorders by magnetic resonance imaging. *Neurol Sci* 2003; 24(suppl 1):S35–S37
18. Koyama M, Yagishita A, Nakata Y, Hayashi M, Bandoh M, Mizutani T. Imaging of corticobasal degeneration syndrome. *Neuroradiology* 2007; 49:905–912
19. Schrag A, Good CD, Miszkiel K, et al. Differentiation of atypical parkinsonian syndromes with routine MRI. *Neurology* 2000; 54:697–702
20. Tripathi M, Dhawan V, Peng S, et al. Differential diagnosis of parkinsonian syndromes using F-18 fluorodeoxyglucose positron emission tomography. *Neuroradiology* 2013; 55:483–492
21. Teune LK, Bartels AL, de Jong BM, et al. Typical cerebral metabolic patterns in neurodegenerative brain diseases. *Mov Disord* 2010; 25:2395–2404
22. Brooks DJ, Seppi K; Neuroimaging Working Group on MSA. Proposed neuroimaging criteria for the diagnosis of multiple system atrophy. *Mov Disord* 2009; 24:949–964
23. Mascalchi M, Vella A, Ceravolo R. Movement disorders: role of imaging in diagnosis. *J Magn Reson Imaging* 2012; 35:239–256
24. Lee WH, Lee CC, Shyu WC, Chong PN, Lin SZ. Hyperintense putaminal rim sign is not a hallmark of multiple system atrophy at 3T. *AJNR* 2005; 26:2238–2242
25. Watanabe H, Saito Y, Terao S, et al. Progression and prognosis in multiple system atrophy: an analysis of 230 Japanese patients. *Brain* 2002; 125:1070–1083
26. Eckert T, Barnes A, Dhawan V, et al. FDG PET in the differential diagnosis of parkinsonian disorders. *Neuroimage* 2005; 26:912–921
27. Boeve BF. Progressive supranuclear palsy. *Parkinsonism Relat Disord* 2012; 18(suppl 1):S192–S194
28. Zhao P, Zhang B, Gao S. ^{18}F-FDG PET study on the idiopathic Parkinson's disease from several parkinsonian-plus syndromes. *Parkinsonism Relat Disord* 2012; 18(suppl 1):S60–S62
29. Kato N, Arai K, Hattori T. Study of the rostral midbrain atrophy in progressive supranuclear palsy. *J Neurol Sci* 2003; 210:57–60
30. Righini A, Antonini A, De Notaris R, et al. MR imaging of the superior profile of the midbrain: differential diagnosis between progressive supranuclear palsy and Parkinson disease. *AJNR* 2004; 25:927–932
31. van den Bogaard SJ, Kruit MC, Dumas EM, Roos

RA. Eye-of-the-tiger-sign in a 48 year healthy adult. *J Neurol Sci* 2014; 336:254–256

32. Kataoka H, Tonomura Y, Taoka T, Ueno S. Signal changes of superior cerebellar peduncle on fluid-attenuated inversion recovery in progressive supranuclear palsy. *Parkinsonism Relat Disord* 2008; 14:63–65
33. Rapinesi C, Serata D, Del Casale A, et al. Depressive pseudodementia in the elderly: effectiveness of electroconvulsive therapy. *Int J Geriatr Psychiatry* 2013; 28:435–438
34. Su L, Cai Y, Xu Y, Dutt A, Shi S, Bramon E. Cerebral metabolism in major depressive disorder: a voxel-based meta-analysis of positron emission tomography studies. *BMC Psychiatry* 2014; 14:321
35. Lajoie C, Levasseur MA, Paquet N. Complete normalization of severe brain ^{18}F-FDG hypometabolism following electroconvulsive therapy in a major depressive episode. *Clin Nucl Med* 2013; 38:735–736
36. Henry ME, Schmidt ME, Matochik JA, Stoddard EP, Potter WZ. The effects of ECT on brain glucose: a pilot FDG PET study. *J ECT* 2001; 17:33–40
37. Clapp AJ, Hunt CH, Johnson GB, Peller PJ. Semiquantitative analysis of brain metabolism in patients with paraneoplastic neurologic syndromes. *Clin Nucl Med* 2013; 38:241–247
38. Darnell RB, Posner JB. Paraneoplastic syndromes involving the nervous system. *N Engl J Med* 2003; 349:1543–1554
39. Graus F, Delattre JY, Antoine JC, et al. Recommended diagnostic criteria for paraneoplastic neurological syndromes. *J Neurol Neurosurg Psychiatry* 2004; 75:1135–1140
40. Sureka J, Jakkani RK. Clinico-radiological spectrum of bilateral temporal lobe hyperintensity: a retrospective review. *Br J Radiol* 2012; 85:e782–e792
41. Masangkay N, Basu S, Moghbel M, Kwee T, Alavi A. Brain ^{18}F-FDG-PET characteristics in patients with paraneoplastic neurological syndrome and its correlation with clinical and MRI findings. *Nucl Med Commun* 2014; 35:1038–1046
42. Caobelli F, Cobelli M, Pizzocaro C, Pavia M, Magnaldi S, Guerra UP. The role of neuroimaging in evaluating patients affected by Creutzfeldt-Jakob disease: a systematic review of the literature. *J Neuroimaging* 2015; 25:2–13
43. Kropp S, Schulz-Schaeffer WJ, Finkenstaedt M, et al. The Heidenhain variant of Creutzfeldt-Jakob disease. *Arch Neurol* 1999; 56:55–61
44. Appleby BS, Appleby KK, Crain BJ, Onyike CU, Wallin MT, Rabins PV. Characteristics of established and proposed sporadic Creutzfeldt-Jakob disease variants. *Arch Neurol* 2009; 66:208–215
45. Kallenberg K, Schulz-Schaeffer WJ, Jastrow U, et al. Creutzfeldt-Jakob disease: comparative analysis of MR imaging sequences. *AJNR* 2006; 27:1459–1462
46. Zhang Y, Minoshima S, Vesselle H, Lewis DH. A case of Creutzfeldt-Jakob disease mimicking corticobasal degeneration: FDG PET, SPECT, and MRI findings. *Clin Nucl Med* 2012; 37:e173–e175
47. Comunale JP Jr, Heier LA, Chutorian AM. Juvenile form of Huntington's disease: MR imaging appearance. *AJR* 1995; 165:414–415
48. Walker FO. Huntington's disease. *Semin Neurol* 2007; 27:143–150
49. Kremer B, Goldberg P, Andrew SE, et al. A worldwide study of the Huntington's disease mutation: the sensitivity and specificity of measuring CAG repeats. *N Engl J Med* 1994; 330:1401–1406
50. Walker FO. Huntington's disease. *Lancet* 2007; 369:218–228
51. Feigin A, Zgaljardic D. Recent advances in Huntington's disease: implications for experimental therapeutics. *Curr Opin Neurol* 2002; 15:483–489
52. Schapiro M, Cecil KM, Doescher J, Kiefer AM, Jones BV. MR imaging and spectroscopy in juvenile Huntington disease. *Pediatr Radiol* 2004; 34:640–643
53. Ciarmiello A, Cannella M, Lastoria S, et al. Brain white-matter volume loss and glucose hypometabolism precede the clinical symptoms of Huntington's disease. *J Nucl Med* 2006; 47:215–222
54. Rosas HD, Feigin AS, Hersch SM. Using advances in neuroimaging to detect, understand, and monitor disease progression in Huntington's disease. *NeuroRx* 2004; 1:263–272
55. Shin H, Kim MH, Lee SJ, et al. Decreased metabolism in the cerebral cortex in early-stage Huntington's disease: a possible biomarker of disease progression? *J Clin Neurol* 2013; 9:21–25
56. Kuhl DE, Markham CH, Metter EJ, Riege WH, Phelps ME, Mazziotta JC. Local cerebral glucose utilization in symptomatic and presymptomatic Huntington's disease. *Res Publ Assoc Res Nerv Ment Dis* 1985; 63:199–209
57. Andrews TC, Weeks RA, Turjanski N, et al. Huntington's disease progression. PET and clinical observations. *Brain* 1999; 122:2353–2363

(Figures start on next page)

FOR YOUR INFORMATION

The reader's attention is directed to part 1 accompanying this article, titled "Multimodality Imaging of Neurodegenerative Processes: Part 1, The Basics and Common Dementias," which begins on page 871.

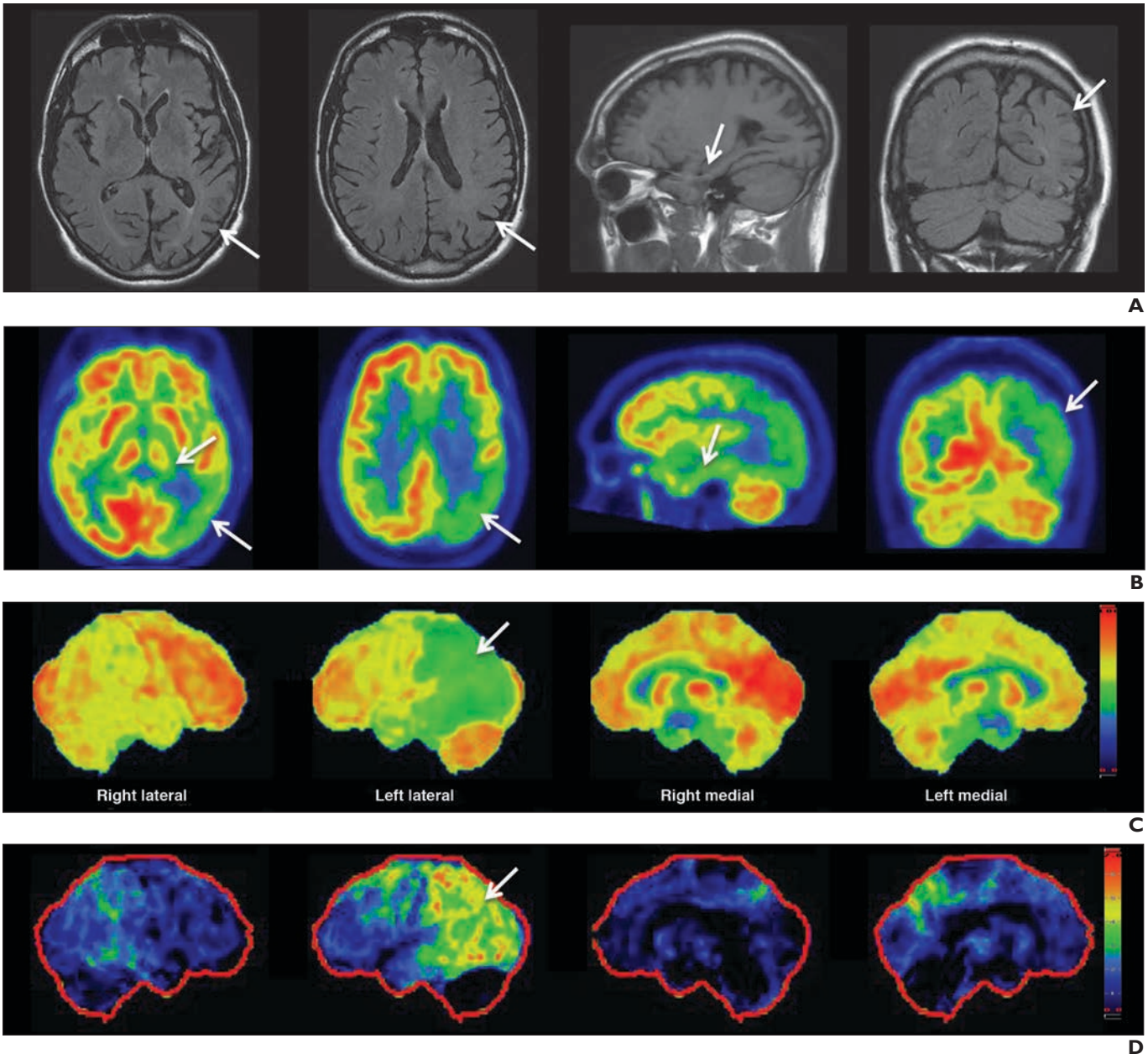

Fig. 1—Corticobasal degeneration in 67-year-old man who presented with cognitive decline, expressive aphasia, right upper extremity rigidity, and focal myoclonus.
A, Axial (*left image* and *middle left image*), sagittal (*middle right image*), and coronal (*right image*) T2-weighted FLAIR MR images show asymmetric cortical atrophy in left temporal and parietal lobes (*arrows*).
B, Axial (*left image* and *middle left image*), sagittal (*middle right image*), and coronal (*right image*) FDG PET images reveal marked left temporoparietal hypometabolism with subtle decreased activity in left basal ganglia (*arrows*).
C and **D,** Three-dimensional stereotactic surface projection (SSP) maps (**C**) and Z-score maps (**D**) confirm severe left-sided cortical hypometabolism (> 5 SD; *arrows*). Three-dimensional SSP images are semiquantitative sampling of metabolism from various cortical locations. Z-score images compare cortical metabolism with age-matched normative database; color change is based on reduction in metabolism relative to number of SDs from mean. For further explanation, see text.

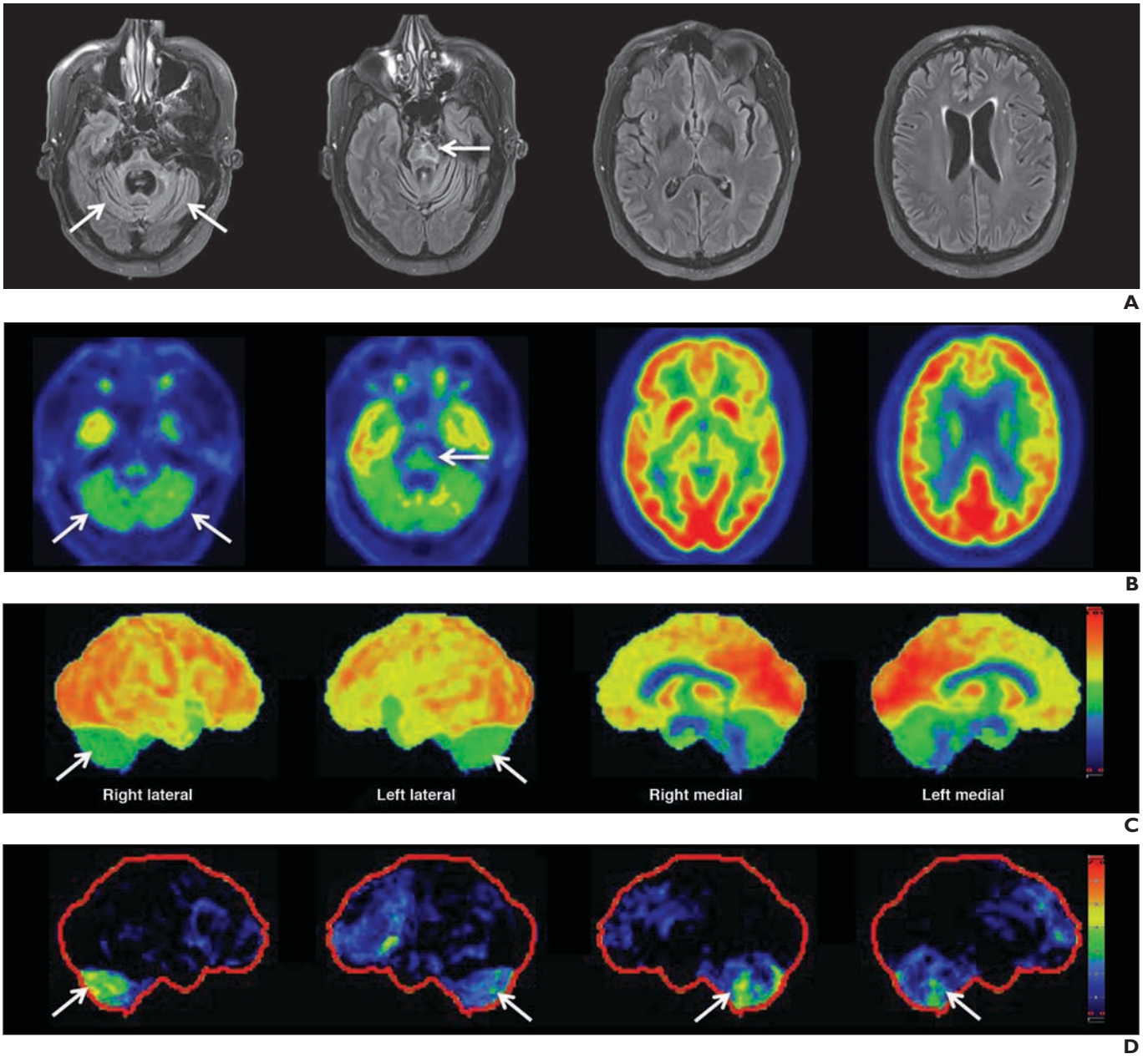

Fig. 2—Multiple-system atrophy (MSA-C) in 56-year-old man who presented with mild parkinsonism, cerebellar ataxia, and autonomic dysfunction.
A, Axial T2-weighted FLAIR images (*images from left to right*: skull base to vertex) show marked focal atrophy of midbrain and both middle cerebral peduncles, ex vacuo dilatation of fourth ventricle, and "hot cross bun" sign with cruciform T2 hyperintensity in pons (*arrows*).
B–D, Axial FDG PET images (*images from left to right* [**B**]: skull base to vertex), 3D stereotactic surface projection maps (**C**), and Z-score projection maps (**D**) show dominant cerebellar and mild pontine hypometabolism (*arrows*) typical of subtype of MSA with predominantly cerebellar ataxia symptoms.

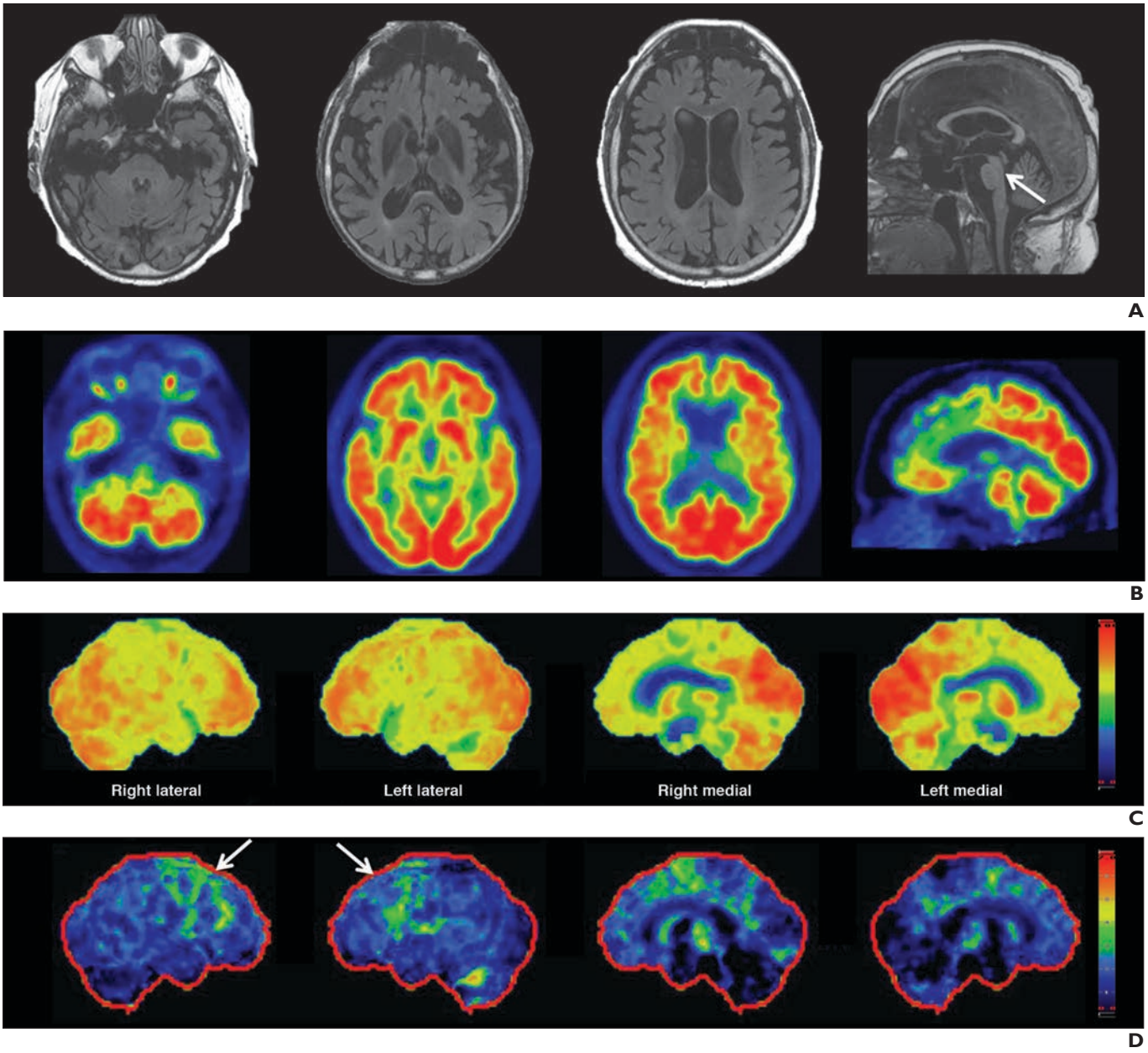

Fig. 3—Progressive supranuclear palsy in 76-year-old woman who presented with bradykinesia, rigidity, postural instability, and pseudobulbar syndrome.
A, Axial T2-weighted FLAIR images (*first three images from left to right*: skull base to vertex) and sagittal T1-weighted image (*right image*) show generalized cerebral atrophy is more prominent in frontotemporal lobes including hippocampi and perisylvian regions. Selective atrophy of midbrain tegmentum with relative preservation of pons (*arrow*), which is termed "hummingbird" sign, is seen on sagittal image.
B and **C,** Axial FDG PET images (*first three images from left to right*, **B**), sagittal FDG PET image (*right image*, **B**), and sagittal 3D stereotactic surface projection maps (**C**) show subtle posterior frontal cortex hypometabolism.
D, Posterior frontal cortex hypometabolism (*arrows*) is better delineated on sagittal Z-score maps.

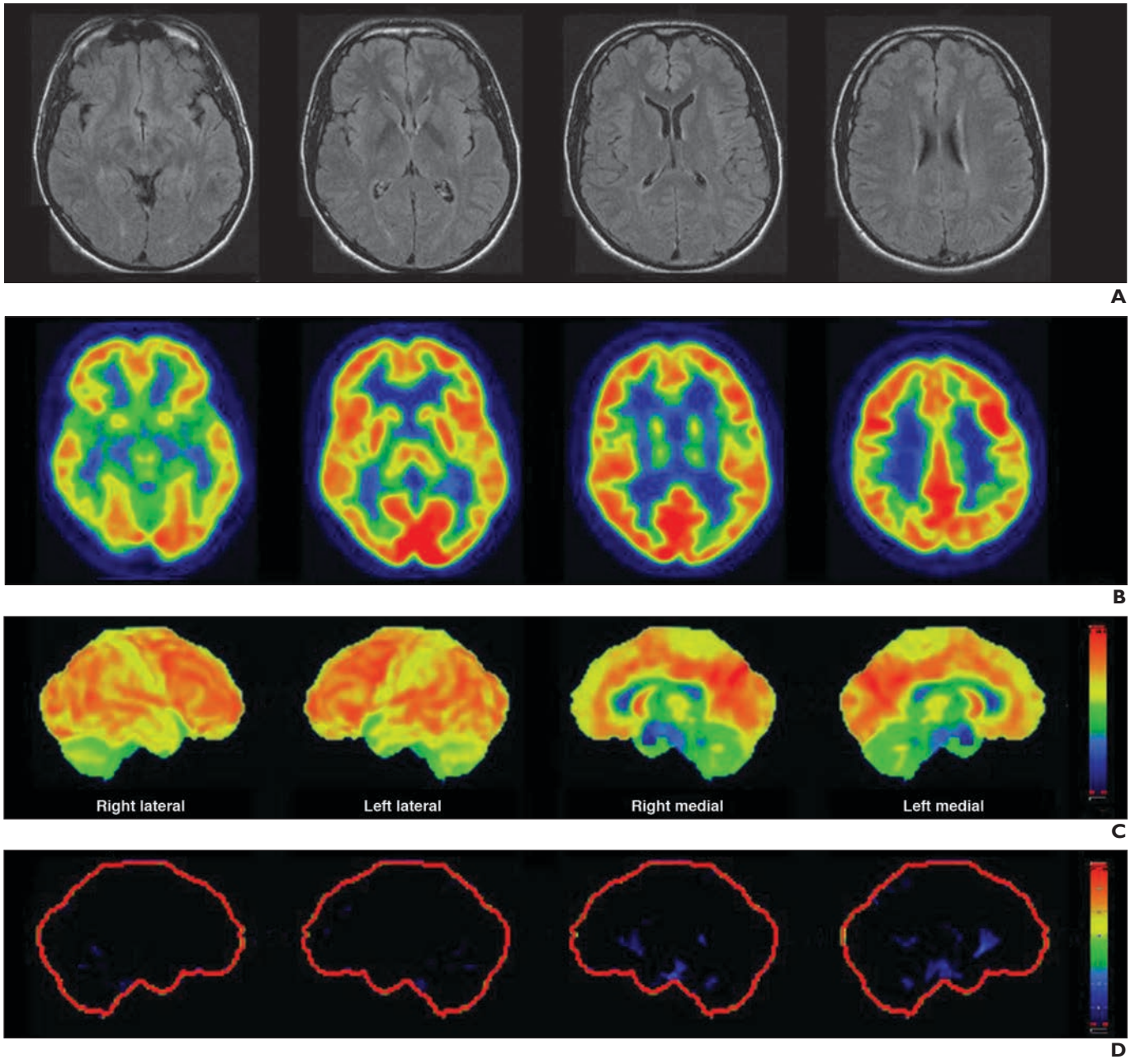

Fig. 4—Pseudodementia in 57-year-old woman who presented with progressive cognitive decline and history of depression.
A–D, Axial FLAIR MR images (*images from left to right* [**A**]: base to vertex), axial FDG PET images (**B**), 3D stereotactic surface projection maps (**C**), and sagittal Z-score maps (**D**) show normal findings. Both MRI and PET studies show normal findings. Nonspecific pattern of diffuse cortical hypometabolism can be seen with pseudodementia.

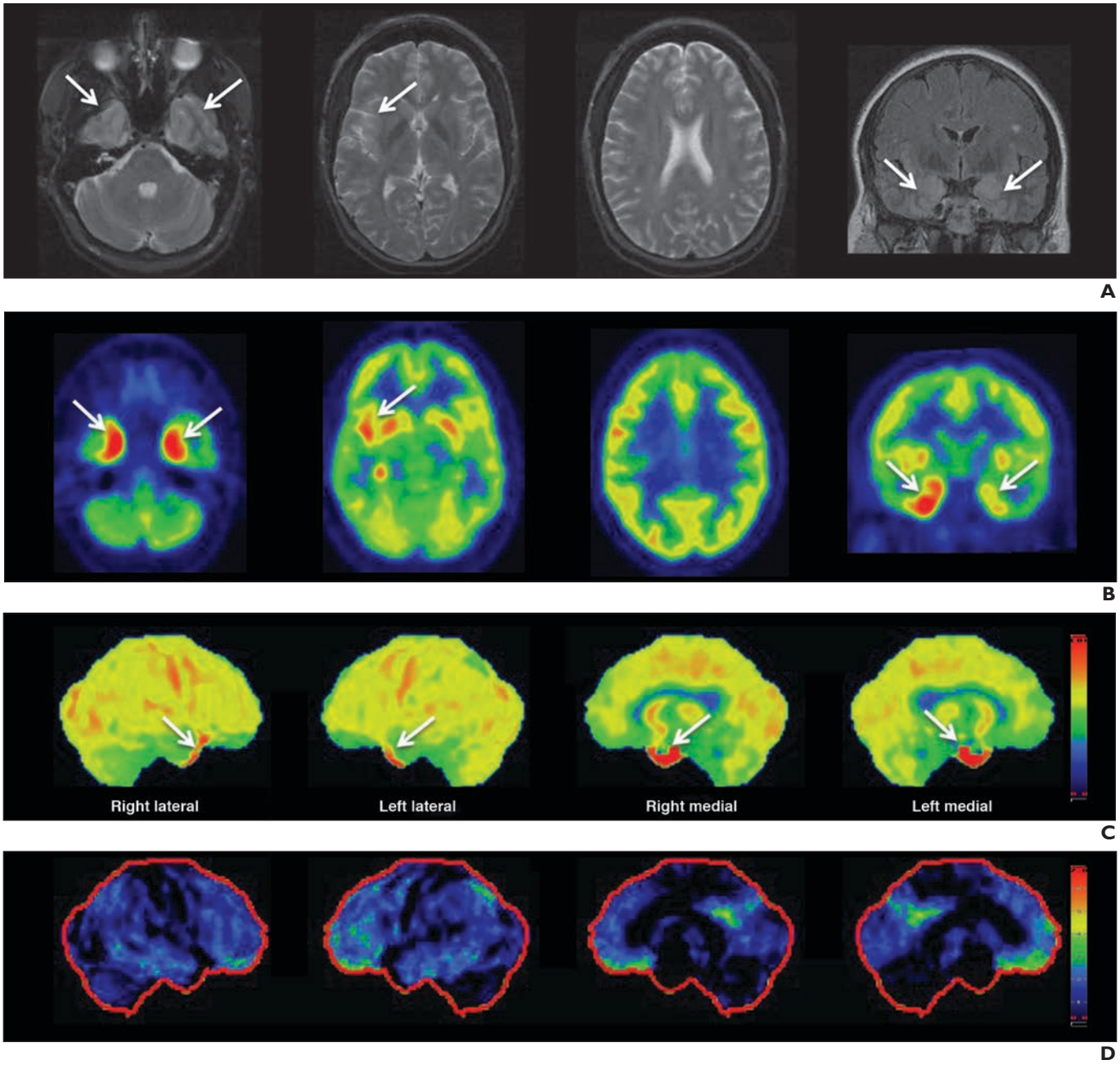

Fig. 5—Paraneoplastic limbic encephalitis in 35-year-old woman who presented with subacute memory deficits and psychiatric symptoms including paranoia and hallucinations.
A, Axial T2-weighted (*first three images from left to right*: base to vertex) and coronal T2-weighted FLAIR (*right image*) MRI shows signal abnormalities in both mesial temporal lobes (*arrows*).
B and **C,** Axial FDG PET images (*first three images from left to right* [**B**]: base to vertex), coronal FDG PET image (*right image*, **B**), and 3D stereotactic surface projection maps (**C**) show mild diffuse cortical hypometabolism and intense hypermetabolism in medial temporal lobes (*arrows*).
D, There is no use for Z-score maps in this patient because they show areas of cortical hypometabolism in patients with neurodegenerative disorders.

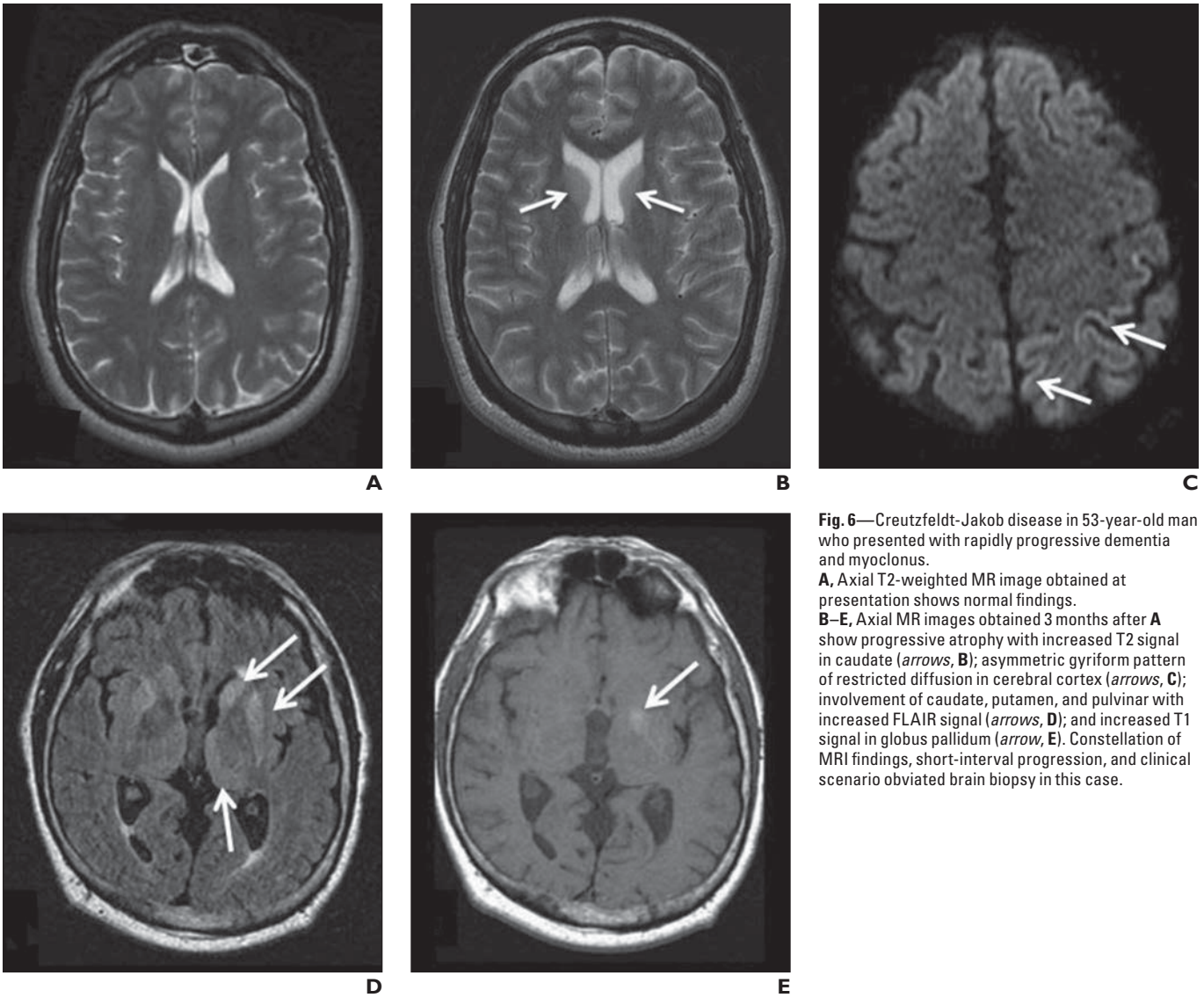

Fig. 6—Creutzfeldt-Jakob disease in 53-year-old man who presented with rapidly progressive dementia and myoclonus.
A, Axial T2-weighted MR image obtained at presentation shows normal findings.
B–E, Axial MR images obtained 3 months after **A** show progressive atrophy with increased T2 signal in caudate (*arrows*, **B**); asymmetric gyriform pattern of restricted diffusion in cerebral cortex (*arrows*, **C**); involvement of caudate, putamen, and pulvinar with increased FLAIR signal (*arrows*, **D**); and increased T1 signal in globus pallidum (*arrow*, **E**). Constellation of MRI findings, short-interval progression, and clinical scenario obviated brain biopsy in this case.

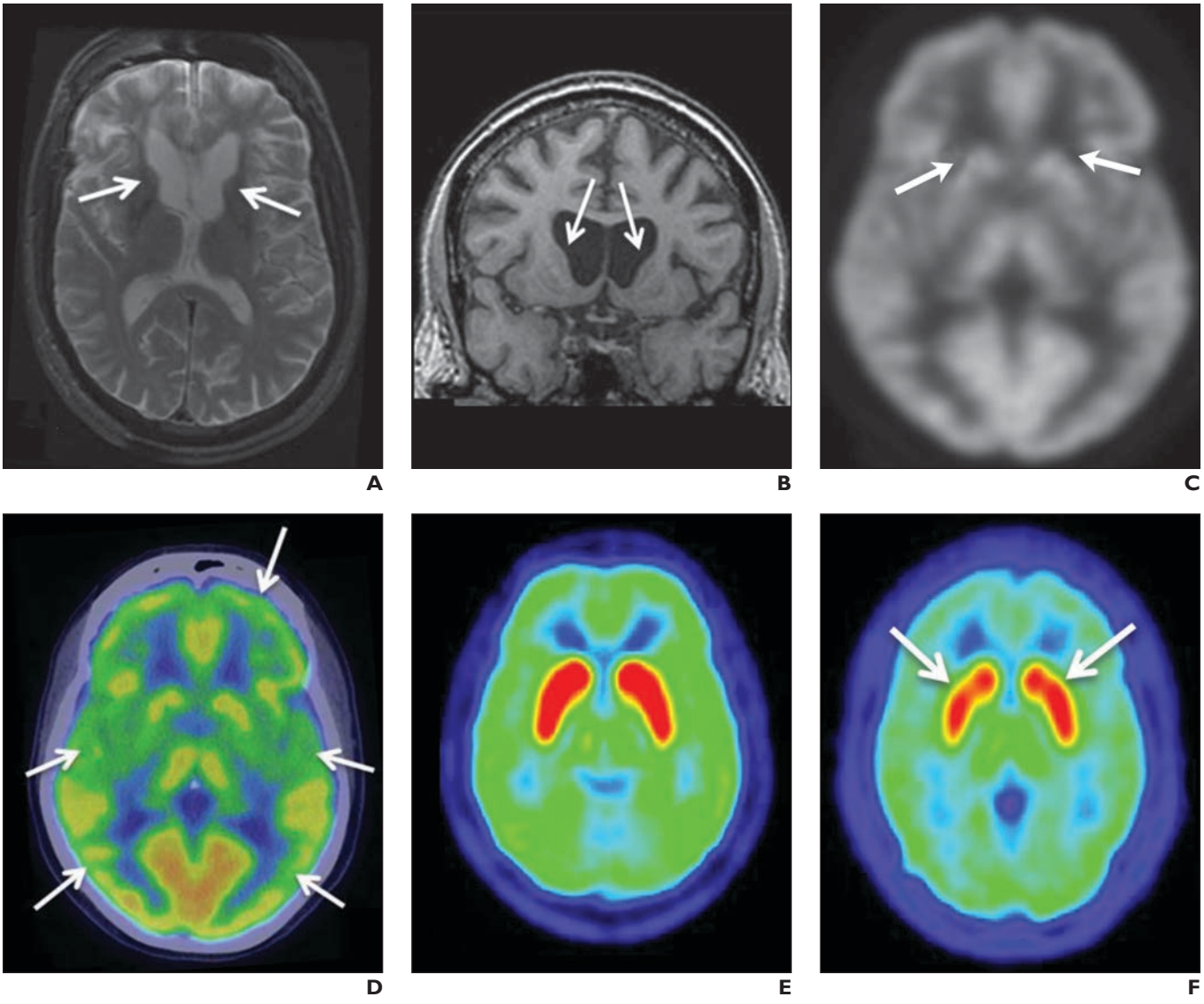

Fig. 7—Huntington disease (HD).
A and **B,** Prominent bilateral caudate atrophy (*arrows*) is visible on axial T2-weighted image (**A**) and coronal T1-weighted image (**B**) of 43-year-old man with HD who presented with choreoathetoid movements.
C, Axial FDG PET image of same patient shown in **A** and **B** reveals subtle decreased uptake in caudate nuclei (*arrows*).
D, Nonspecific pattern of patchy decreased cortical uptake (*arrows*), which is common in patients with HD, is easier to see on this axial FDG PET/CT color-scale image of same patient shown in **A**–**C**.
E and **F,** Axial ^{11}C-raclopride PET images of 34-year-old control patient (**E**) and 32-year-old presymptomatic HD gene carrier (**F**). Decreased uptake is seen in basal ganglia of gene carrier (*arrows*, **F**). (Courtesy of Center for Neuroscience, The Feinstein Institute for Medical Research, Northwell Health, Manhasset, NY).